



Microcalorimeter Absorber Optimization for ATHENA and LEM

Edward Wassell¹ · Joseph Adams^{1,2} · Simon Bandler¹ · James Chervenak¹ ·
Renata Cumbee¹ · Fred Finkbeiner^{1,3} · Joshua Fuhrman^{1,2} · Samuel Hull^{1,4} ·
Richard Kelley¹ · Caroline Kilbourne¹ · Jennette Mateo¹ · Haruka Muramatsu^{1,5} ·
Frederick Porter¹ · Asha Rani^{1,6} · Kazuhiro Sakai^{1,2} · Stephen Smith¹ ·
Nicholas Wakeham^{1,2} · Sang Yoon^{1,6}

Received: 3 November 2023 / Accepted: 9 June 2024 / Published online: 18 June 2024
This is a U.S. Government work and not under copyright protection in the US; foreign copyright protection
may apply 2024

Abstract

High quantum efficiency (QE) X-ray absorbers are needed for future X-ray astrophysics telescopes. The Advanced Telescope for High ENergy Astrophysics (ATHENA) mission requirements for the X-ray Integral Field Unit (X-IFU) instrument dictate, at their most stringent, that the absorber achieve vertical QE > 90.6% at 7 keV and low total heat capacity, 0.731 pJ/K. The absorber we have designed is 313 μm square composed of 1.05 μm Au and 5.51 μm electroplated Bi films (Barret et al. in *Exp Astron* 55:373–426, 2023). Overhanging the TES, the absorber is mechanically supported by 6 small legs whose 5 μm diameter is tuned to the target thermal conductance for the device. Further requirements for the absorber for X-IFU include a > 40% reflectance at wavelengths from 1 to 20 μm to reduce shot noise from infrared radiation from higher temperature stages in the cryostat. We meet this requirement by capping our absorbers with an evaporated Ti/Au thin film. Additionally, narrow gaps between absorbers are required for high fill fraction, as well as low levels of fine particulate remaining on the substrate and zero shorts between absorbers that may cause thermal crosstalk. The Light Element Mapper (LEM) is an X-ray probe concept optimized to explore the soft X-ray emission from 0.2 to 2.0 keV. These pixels for LEM require high residual resistance ratio (RRR) thin 0.5 μm Au absorbers to thermalize uniformly and narrow < 2 μm gaps between pixels for high areal fill fraction. This paper reports upon technology developments required to successfully yield arrays of pixels for both mission concepts and presents first testing results of devices with these new absorber recipes.

Keywords Transition edge sensor · X-ray microcalorimeter · Superconducting devices

Extended author information available on the last page of the article

1 ATHENA Absorber Fabrication

X-ray absorber structures are integral to the design and performance of the microcalorimeter sensor. Their photolithographic integration enables exquisite determination of such details as thermal time constants and spectral resolution performance but can influence fabrication process flow. While many groups [2–7] have developed processes to fabricate electroplated bismuth absorbers for microcalorimeters, the requirements on X-ray absorbers for the ATHENA X-IFU instrument pose unique fabrication challenges. Specifically, for X-IFU, we need to fabricate free standing absorbers with six narrow 4–5 μm diameter stems supporting a large $313 \mu\text{m}^2$ area absorber composed of 1.05 μm Au and 5.51 μm Bi and capped by a thin Ti/Au coating [1]. The stem diameter is chosen to achieve structural and thermal needs of the absorber while being feasible to fabricate. However, small stem diameter can lead to a mechanically weak stem which may not be suitable for extended geometries and certain film thickness limits. To enhance the structural integrity of the stem, a funnel-shape photoresist mold using a proximity exposure has been developed to control the shape of the stem. Backfilling the stems with electroplated Au were also incorporated to increase the strength of thin stems in supporting the mechanical stresses applied to them from the large absorbers. Additionally, to optimize for post-patterning substrate cleanliness for absorber yield, we have developed a method of plating the thick bismuth absorbers using a photoresist mold while controlling the bismuth grain growth with a leveling process while electroplating. Finally, to separate the pixels from each other, we use an ion mill etch to remove the Ti/Au capping layer as well as the Ti/Au seed layer. Although others have backfilled stems [8] and electroplated bismuth through a photoresist mold [4, 5, 7], we are combining all of these patterning steps, requiring numerous repatterns over the sacrificial resist layer supporting the electroplated mushroom absorber overhanging the TES. Figure 1 has a cartoon of the pixel architecture (Left) and a table listing our process fabrication steps (Right).

Historically, our calorimeter group first developed a procedure to yield overhanging mushroom shaped X-ray absorbers with electroplated gold and bismuth films suspended above a transition edge sensor on a silicon nitride membrane [9, 10]. Our NASA group has demonstrated an average 2.25 eV energy resolution in prototype arrays of spectrometer pixels with average thicknesses of 1.5 μm Au + 3.0 μm Bi absorbers on 275 μm pitch [11]. As the bismuth films are rough, the thicknesses reported are averages calculated by differential weighing and calibrated by optical interferometry and SEM measurements [12]. Recently revised ATHENA requirements for lower heat capacity and higher quantum efficiency imposed a fabrication change to thinner Au (1.0 μm) and thicker Bi (5.5 μm) as well as an increase in absorber pixel size to $313 \mu\text{m}^2$ [1]. Our initial attempts to yield these new absorbers resulted in absorber touches to the substrate degrading pixel performance. Further, some pixels collapse completely when the stems break near the base. SEM imaging revealed that the thinner Au stems filled with bismuth grains were not mechanically strong enough to support the larger area thicker bismuth absorbers. Figure 2 shows examples of absorber collapse (top and bottom left) and hollow stems that can break

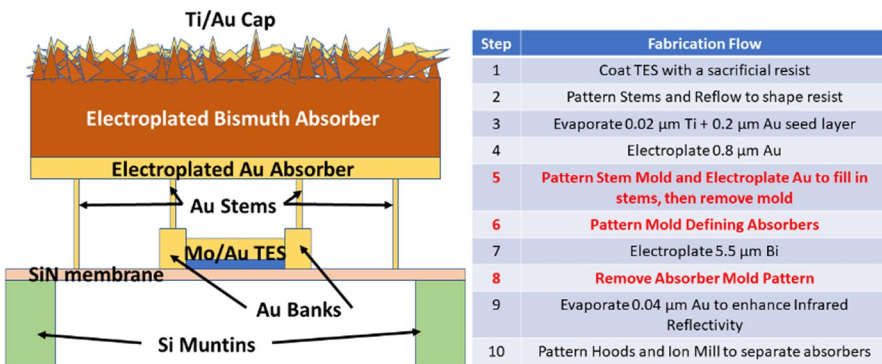


Fig. 1 A cartoon of pixel architecture (left) highlights an X-ray absorber overhanging but thermally linked to a TES by thin stems and suspended above a SiN membrane of low thermal conductance. Absorber fabrication flow is listed (right) with our new process additions in red (Color figure online)

during release (top and bottom right). We measured the film stresses of different layers with respect to the wafer as substrate and found the evaporated Ti/Au seed layer exerts a positive stress on the underlying sacrificial photoresist layer, the electroplated gold is mostly stress free, and the bismuth film is compressive, curving the wafer downward (see appendix). With hollower stems from thinner electroplated Au and the additional stress from the thicker bismuth film, our traditional stem design was not mechanically strong enough to support the larger area absorbers required by

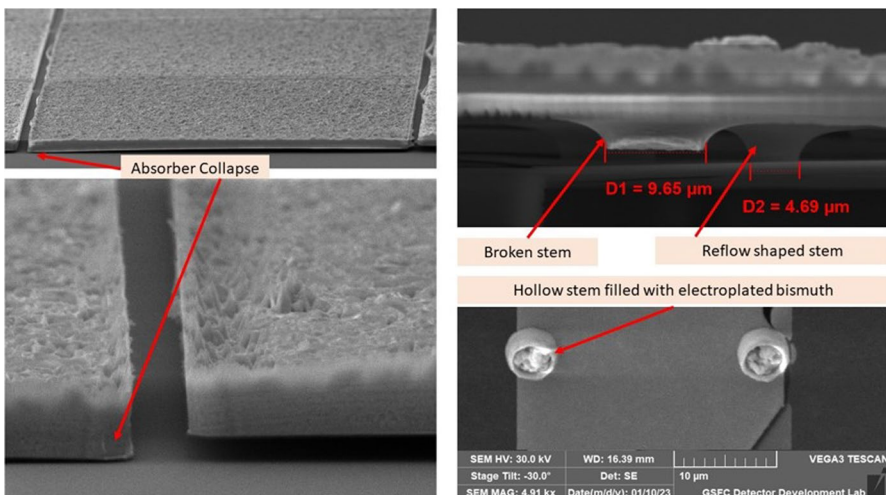


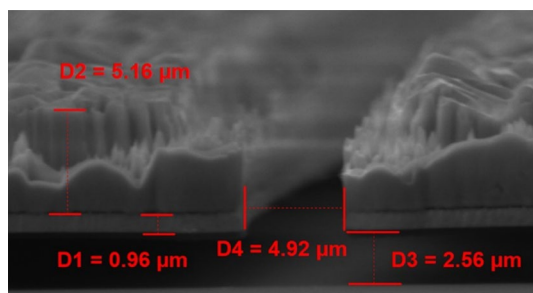
Fig. 2 Initial attempts to meet new ATHENA detector requirements for larger absorbers with thicker bismuth and thinner gold resulted in absorbers touching the substrate (top and bottom left), and broken stems (top and bottom right). Compressive stresses in the thicker bismuth film shape the absorbers down at the corners

ATHENA. Further, the thicker bismuth film led to absorbers curving down at the corners and in some cases touching the substrate.

Our solution to making mechanically stable absorbers was threefold. First, we smoothed the shape of stems using a double exposure of the resist and a reflow bake. Our standard reflow bake caused the resist to flow toward the developed stems leaving an elevated rim of resist around the stem. Adding a proximity exposure to our standard hard exposure yielded smooth conical shaped stems after the reflow bake which is necessary to harden the resist, so it does not flow underneath the seed and plated metal layers. Next, we increased the titanium thickness of the seed layer deposition to counteract the compressive stress of the bismuth. Third, we pattern atop the seed layer and backfill the stems with electroplated Au to make them mechanically more robust.

While developing our new process to mechanically strengthen the stems supporting the overhanging absorbers, we also worked out a procedure to electroplate the absorbers through a photoresist mold. Previously, we have defined our absorbers by a long ion mill through the entire Au/Bi stack. Because the Bi grain size increases with thickness [2], we have found that after a long ion mill, a fraction of absorbers have small metal bridges thermally shorting them together, degrading badly the energy resolution in the affected pixels. Electroplating the bismuth through a photoresist mold and then following with a much shorter ion mill to clear the remaining Ti/Au from both the capping and seed layers appears to solve the problem of thermally shorted pixels. To ensure that the streets clear, the pattern for the ion mill step in our first attempt ended up wider than the streets by about 2 μm resulting in some ion milling of the bismuth at the edges of the absorber leaving a step. We are actively working on reducing the width of this step. Figure 1 (Right) details our new fabrication flow with the additional steps highlighted in red. As will be shown later in this paper, despite the complications from the additional fabrication steps, our first delivered devices showed no degradation in energy resolution, no additional broadening in the low energy tails of the X-ray spectrum, and we were still able to achieve the desired heat capacity. Figure 3 shows SEM images of an array that yielded after electroplating Bi through a photoresist mold. The absorbers are free standing and flat with 5.0 μm gaps between pixels

Fig. 3 SEM image of a prototype ATHENA absorber incorporating electroplating Bi through a mold and backfilling the stems. We achieved flat free standing absorbers with 5.2 μm thick Bi atop 1.0 μm thin Au while preserving 5.0 μm gaps between pixels (Color figure online)



2 LEM Absorber Fabrication

Absorber fabrication for LEM follows a similar flow to ATHENA without the added bismuth. The proposed LEM focal plane is a hybrid array consisting of two different pixel types. The inner array has 784 single high resolution pixels, and the outer array consists of 3184 four pixel hydras, consisting of a single transition edge sensor (TES) connected to four absorber pixels by different thermal links. Each distinct event can be separated algorithmically according to its pulse height and rise time [13]. These hydras for LEM require high residual resistance ratio (RRR) 0.5 μ m Au absorbers to thermalize uniformly. Yielding flat thin Au absorbers with narrow 1.5 μ m gaps between pixels poses its own fabrication challenges. Thin (0.5 μ m) large area Au absorbers are difficult to yield because film stresses in the Titanium adhesion layer tend to curl the absorbers up at the corners [14]. While other groups have proposed corrugations in the absorber to mitigate these stresses and keep the absorbers flat [8], our solution was to reduce the Ti adhesion layer thickness and add the stem backfilling process to strengthen the mechanical support to the substrate.

The first attempt at yielding absorbers for LEM resulted in the loss of a handful of pixels during the release of the wafers. Figure 4 shows the missing absorbers after release. Photolithography was able to achieve narrow 1.5 μ m gaps between absorber pixels for high areal fill factor. The SEM images in Fig. 4 highlight the success of yielding 0.5 μ m thin Au absorbers with narrow gaps despite the mechanical stresses that lead to curvature in the absorber. Reduction in the thickness of the titanium adhesion layer from 10 to 2.5 nm changed the profile of the absorbers from curling up to curling down at the corners. Inspecting areas of the array where pixels were

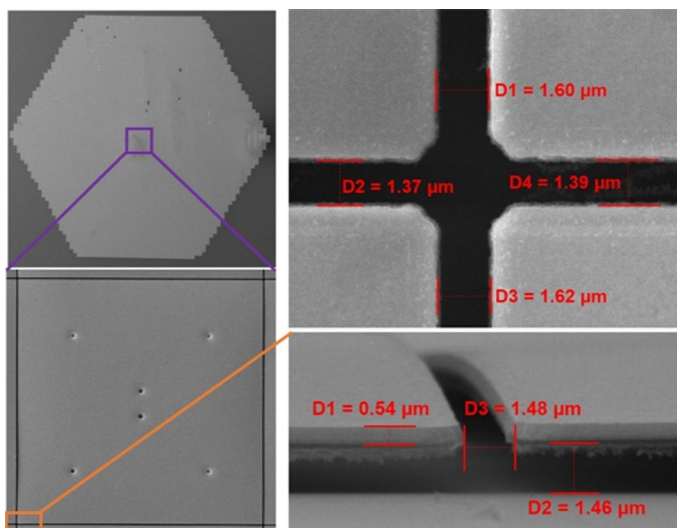


Fig. 4 SEM images of LEM. Top left the hexagonal detector array. Bottom left a single pixel with six funnel shaped stems. Top right yield of absorbers with under 2 μ m gaps. Bottom right edge view of curvature in the absorbers. A thin skirt of material left from ion mill sputtering of absorber metal into the sacrificial photoresist can be seen underhanging the absorbers

lost, we discovered cracks near the base of the stems visible in Fig. 5. Since the base of the stem is nominally 4 μm and widens considerably through our photoresist reflow process, electroplating 0.5 μm of Au will leave the stems hollow. Our initial fabrication run did not include backfilling the stems, which has been shown to eliminate the absorber loss.

After coating the shaped stem mold resist with a Ti/Au seed layer, we developed a process to backfill the hollow stem area with electroplated Au to make the absorbers mechanically robust without significantly increasing the heat capacity of the absorbers. Careful process control is needed to ensure the plating does not overfill the thin stems and form pillars on the absorbers. Figure 6 shows Keyence optical imaging of the surface of the Au coated stem photoresist mold and the depth profile of a stem before (top) and after (bottom) the stem filling electroplating procedure. The initial 4.3 μm stem height agrees with the mold resist thickness measured by a stylus profilometer. Figure 6 bottom shows that three microns of the stem have been backfilled, allowing room to tune this process further.

3 ATHENA Detector Results

We tested the ATHENA detectors with the new absorber method and found no performance degradation. Eleven pixels from two wafers with the old absorber method and five pixels from one wafer with the new absorber method were examined. The Au in the absorbers is a combination of 0.2 μm evaporated Au as a seed layer for electroplating, 0.8 μm electroplated Au and then a 0.04 μm capping evaporated Au over the bismuth to increase infrared reflectivity. The pixels tested vary in width of the TES thin film but are from the same location on each wafer and are otherwise comparable. Heat capacities from both absorber methods are consistent with the predicted values from the TES and absorber dimensions. Using an Fe55 source to illuminate the detector, the energy resolution for a single pixel is found to be 1.92 eV as shown in an Mn-K α spectrum in Fig. 7.

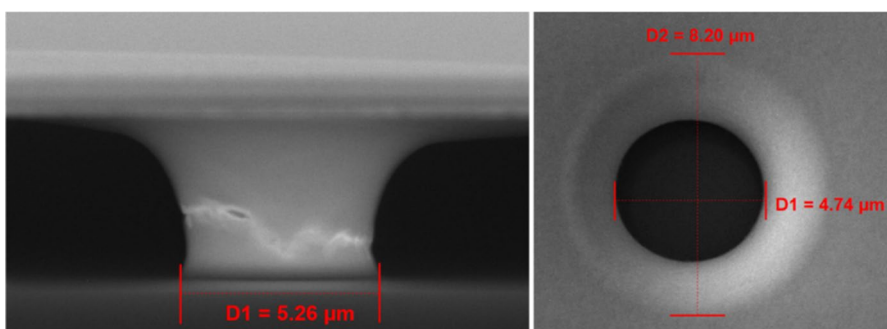


Fig. 5 Edge-on SEM image (left) shows a stem that cracked at the base due to high mechanical stresses from the thin absorber. Our improved photolithography with reflow (right) yields a smooth funnel shaped stem

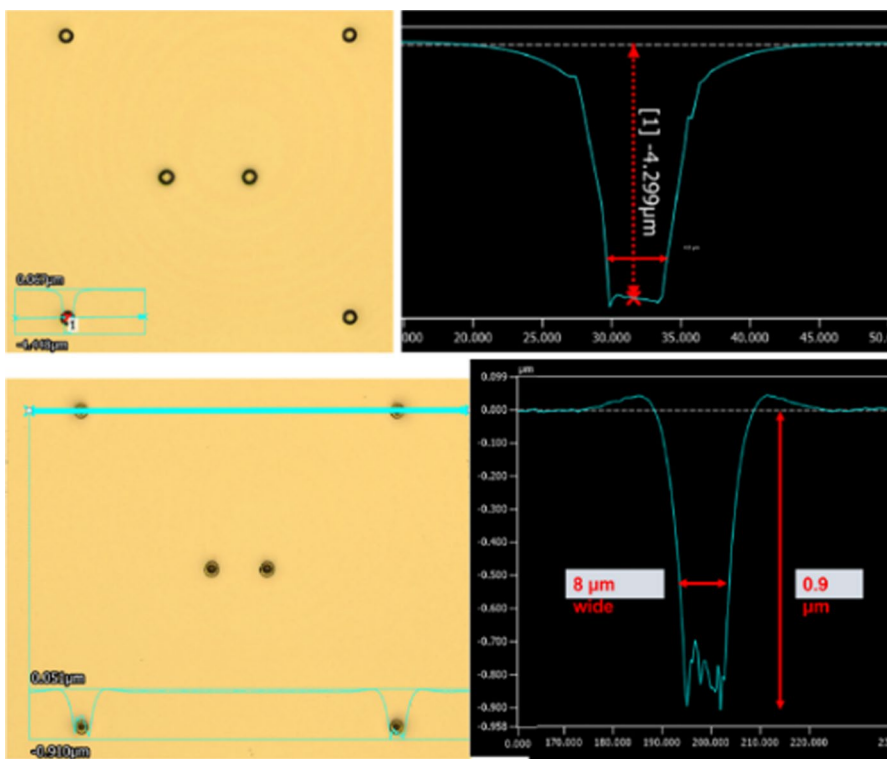


Fig. 6 Keyence image and measurement of a single stem before (top) and after (bottom) backfilling the stem with electroplated Au

4 Appendix Absorber Film Stress

ATHENA absorbers from bottom to top include thin film layers of Titanium, evaporated Au, electroplated Au, electroplated Bismuth, evaporated Titanium and evaporated Au. Film stresses were measured using an FSM film stress measurement tool. A baseline measurement mapping on the wafer with six line scans each offset by 60 degrees was taken prior to evaporation of the bottom Ti/Au seed layer and compared with a second mapping after the Ti/Au seed layer evaporation. This measurement was always positive in value, between +30 and +60 MPa, when the titanium seed was 20 nm thick, indicating a straining of the underlying sacrificial photoresist layer. Previous attempts to yield thin all Au absorbers using this seed layer resulted in absorbers curling up at the corners [14]. Next, a new baseline was taken prior to electroplating the Au film and compared with a mapping of the wafer after the Au electroplating was complete. The electroplated Au film was found on average to be stress free. For the electroplated bismuth film, we took the baseline measurement and second mapping after the bismuth electroplating with the wafer face down to avoid line scans on the rough bismuth surface.

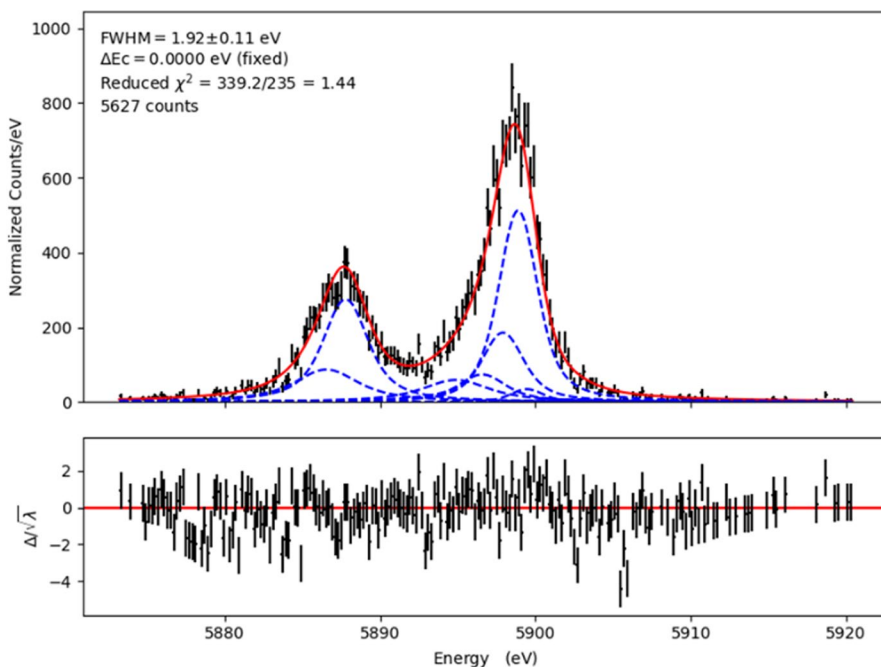


Fig. 7 With the new absorber fabrication method, we have achieved sub 2 eV energy resolution on a pixel from an ATHENA prototype array illuminated by an Fe55 source for the Mn-K α line in an x-ray spectrum

The measured stress on the backside of the silicon wafer from the electroplated film was positive between +1 and +8 MPa, indicating that the bismuth film is compressing the substrate underneath. Thus, in terms of the absorber, the titanium film tends to cause the Au to curl upwards at the corners. The bismuth film exerts a compressive force and tends to cause the absorbers to curl down at the corners. These data drove our decision to increase the Titanium seed layer film thickness for our ATHENA absorbers, and decrease it for the thinner all Au LEM absorbers.

Author contributions E.J. Wassell wrote the main manuscript text with help from J.A. Chervenak. E.J. Wassell prepared figures 1–6. J. Fuhrman provided the text for the Results sect. 3 of the manuscript and provided figure 7 for the manuscript. All authors reviewed the manuscript.

Funding The material is based upon work supported by NASA under award number 80GSFC21M0002 and additionally by funding through Goddard Space Flight Center task 244904.04.10.01.02.02.

Declarations

Conflict of interest The authors declare no conflict of interest.

Open Access This article is licensed under a Creative Commons Attribution 4.0 International License, which permits use, sharing, adaptation, distribution and reproduction in any medium or format, as long as you give appropriate credit to the original author(s) and the source, provide a link to the Creative Commons licence, and indicate if changes were made. The images or other third party material in this article are included in the article's Creative Commons licence, unless indicated otherwise in a credit line to the material. If material is not included in the article's Creative Commons licence and your intended use is not permitted by statutory regulation or exceeds the permitted use, you will need to obtain permission directly from the copyright holder. To view a copy of this licence, visit <http://creativecommons.org/licenses/by/4.0/>.

References

1. D. Barret et al., *Exp. Astron.* **55**, 373–426 (2023). <https://doi.org/10.1007/s10686-022-09880-7>
2. L.M. Gades et al., *IEEE Trans. Appl. Supercond.* **27**, 1–5 (2017). <https://doi.org/10.1109/TASC.2017.2662007>
3. D. Yan et al., *IEEE Trans. Appl. Supercond.* **31**, 1–5 (2021). <https://doi.org/10.1109/TASC.2021.3059972>
4. J. Weber et al., *Supercond. Sci. Technol.* **33**, 115002 (2020). <https://doi.org/10.1088/1361-6668/abb206>
5. P. Khosropahah et al., *Proc. SPIE* (2018). <https://doi.org/10.1117/12.2313439>
6. J. Chen et al., *Materials* **14**, 7169 (2021). <https://doi.org/10.3390/ma14237169>
7. E.J. Wassell et al., *IEEE Trans. Appl. Supercond.* **27**(4), 1–5 (2017). <https://doi.org/10.1109/TASC.2016.2633783>
8. C.V. Ambarish et al., *IEEE Trans. on Appl. Supercond.* **33**(5), 1–5 (2023). <https://doi.org/10.1109/TASC.2023.3243156>
9. C.A. Kilbourne et al., *Proc. SPIE* **6266**, 626621 (2006). <https://doi.org/10.1117/12.672419>
10. A.D. Brown, *J. Low Temp. Phys.* **151**(1), 413–417 (2008). <https://doi.org/10.1007/s10909-007-9669-2>
11. S.J. Smith et al., *IEEE Trans. on Appl. Supercond.* **25**, 3 (2015). <https://doi.org/10.1109/TASC.2014.2369352>
12. R. Hummatov et al., *J. Low Temp. Phys.* **199**, 393–400 (2020). <https://doi.org/10.1007/s10909-020-02424-3>
13. S.J. Smith et al., *IEEE Trans. Appl. Supercond.* **19**, 451–455 (2009). <https://doi.org/10.1109/TASC.2009.2019557>
14. M.E. Eckart et al., *IEEE Trans. Appl. Supercond.* **23**, 3 (2013). <https://doi.org/10.1109/TASC.2013.2244631>

Publisher's Note Springer Nature remains neutral with regard to jurisdictional claims in published maps and institutional affiliations.

Authors and Affiliations

Edward Wassell¹ · **Joseph Adams**^{1,2} · **Simon Bandler**¹ · **James Chervenak**¹ ·
Renata Cumbee¹ · **Fred Finkbeiner**^{1,3} · **Joshua Fuhrman**^{1,2} · **Samuel Hull**^{1,4} ·
Richard Kelley¹ · **Caroline Kilbourne**¹ · **Jennette Mateo**¹ · **Haruka Muramatsu**^{1,5} ·
Frederick Porter¹ · **Asha Rani**^{1,6} · **Kazuhiro Sakai**^{1,2} · **Stephen Smith**¹ ·
Nicholas Wakeham^{1,2} · **Sang Yoon**^{1,6}

✉ Edward Wassell
edward.wassell@nasa.gov

¹ NASA Goddard Space Flight Center, 8800 Greenbelt Rd, Greenbelt, MD 20771, USA

² Center for Space Sciences and Technology, University of Maryland, Baltimore County, Baltimore, MD 21250, USA

³ Sigma Space Corp./Hexagon US Federal, 4600 Forbes Blvd., Lanham, MD 20706, USA

⁴ Department of Astronomy, University of Maryland, College Park, MD 20742, USA

⁵ The Catholic University of America, Washington, DC 20064, USA

⁶ Science Systems and Applications, Inc. (SSAI), 10210 Greenbelt Rd, Lanham, MD 20706, USA